PHYSICAL REVIEW B **75**, 020509(R) (2007)

Anharmonicity and self-energy effects of the E_{2g} phonon in MgB_2

A. Mialitsin,[1,3] B. S. Dennis,[1] N. D. Zhigadlo,[2] J. Karpinski,[2] and G. Blumberg[1,*]
[1]*Bell Laboratories, Alcatel-Lucent, Murray Hill, New Jersey 07974, USA*
[2]*Solid State Physics Laboratory, ETH, CH-8093 Zürich, Switzerland*
[3]*Department of Physics and Astronomy, Rutgers University, Piscataway, New Jersey 08854, USA*
(Received 4 October 2006; published 11 January 2007)

We present a Raman scattering study of the E_{2g} phonon anharmonicity and of superconductivity-induced self-energy effects in MgB_2 single crystals. We show that anharmonic two-phonon decay is mainly responsible for the unusually large linewidth of the E_{2g} mode. We observe ~2.5% hardening of the E_{2g} phonon frequency upon cooling into the superconducting state and estimate the electron-phonon coupling strength associated with this renormalization.

DOI: 10.1103/PhysRevB.75.020509 PACS number(s): 74.70.Ad, 74.25.Ha, 74.25.Gz, 78.30.Er

High-T_c superconductivity in MgB_2 is known to be promoted mainly due to the boron layers;[1] thus the high-frequency lattice vibrations of light boron atoms beneficially increase the electron-phonon coupling. The E_{2g} Raman-active in-plane boron vibrational mode contributes significantly to superconductivity; this fact is reflected by the Eliashberg function $\alpha^2F(\omega)$ peaking in the same frequency range where a high phononic density of states is accounted for by Van Hove singularities of the E_{2g} branch in the Γ and A points of the Brillouin zone (BZ).[2,3] The reason the E_{2g} mode plays a prominent role in the superconducting (SC) mechanism is that the mode strongly couples to the σ-type states of the boron plane as can be seen from the basic geometry of the electronic configuration.[4]

Raman spectra exhibit unusually broad linewidth of the E_{2g} mode[5–7] which has been the subject of numerous speculations. While high impurity scattering in earlier low-quality samples has been suggested as one of the possible reasons, this mechanism can be readily excluded with recent high-quality single crystals. The two remaining contributions to the E_{2g} phonon rapid decay are (i) strong electron-phonon coupling and (ii) multiphononic decay (subsequently referred to as *anharmonicity*). The relative importance of the electron-phonon coupling and anharmonicity in this matter is under intense debate. On one hand a density functional theory calculation asserts that the anharmonic contribution to the E_{2g} phonon linewidth is negligible (~1 meV).[8] On the other hand analysis of the phonon self-energy in the long-wavelength limit shows that the σ-band contribution to the phonon decay is vanishing.[9] Thus, even when contributions of the spectral weight of $\alpha^2F(\omega)|_{\omega<\omega_{E_{2g}}}$ to the damping of the E_{2g} phonon are accounted for,[10] the experimentally observed linewidth of 25–35 meV at low temperatures[5,6] cannot be explained with electron-phonon coupling alone, whose part in the E_{2g} mode linewidth at low temperatures amounts to about 6 meV even in such an elaborate scenario as that in Ref. 10.

Raman scattering experiments have shown that the frequency of the E_{2g} mode in single crystals at room temperature is around 79 meV,[5,6] whereas theoretical calculations systematically underestimate this value by about 10 meV.[3,8] It has been suggested that if the E_{2g} band around the Γ point is anharmonic then the E_{2g} mode frequency is increased by the missing amount to match the experimentally observed value.[13,14] In addition, the experimentally observed T_c and the reduced isotope effect[12] can only be reconciled within anisotropic strong-coupling theory if the E_{2g} mode anharmonicity is explicitly included.[4,11]

Since the E_{2g} mode is responsible for a significant part of the SC pairing a renormalization of the mode frequency upon entering into the SC phase is expected. Moreover, it was predicted that the mode renormalization along the Γ-A direction of the BZ is particularly strong.[13] The temperature dependence of phonon dispersions has been studied by inelastic x-ray scattering; however, the expected self-energy effects have not been demonstrated.[8,15] In earlier Raman work on single-crystalline MgB_2 a change of linewidth between room temperature and T_c has been observed[6] but not discussed. In the experimental context it is important to notice that single-crystal studies should preferably be considered as a valid gauge of MgB_2 bulk properties because results from powdered, polycrystalline, ceramic, film, wire, etc., samples show significant variations, especially in relation to phonon excitations (compare Refs. 7 and 16).

In this work we provide spectroscopic information on (i) the E_{2g} phonon excitation resonance, (ii) the reasons for the mode's large linewidth, and (iii) the self-energy effects upon entering into the SC state. In particular, (i) by means of the resonant Raman excitation profile (RREP) we show that the light couples to the E_{2g} phonon via σ-π interband transition; (ii) we study the E_{2g} phonon shape as a function of temperature and fit the linewidth temperature dependence with an anharmonic decay model; (iii) we observe the E_{2g} phonon renormalization (mode hardening ~2.5%) upon entering into the SC phase.

Raman scattering from the *ab* surface of MgB_2 single crystals grown as described in Ref. 17 was performed in backscattering geometry using about 1 mW of incident power focused to a 100×200 μm^2 spot. We have collected data from two samples that are denoted as crystal $\mathcal{A}$ and crystal $\mathcal{B}$ when a distinction is necessary. The magnetic field data were acquired with a continuous flow cryostat inserted into the horizontal bore of a SC magnet. The sample temperatures quoted have been corrected for laser heating. We used the excitation lines of a Kr^+ laser and a triple-grating spectrometer for analysis of the scattered light. The data were corrected for the spectral response of the spectrometer

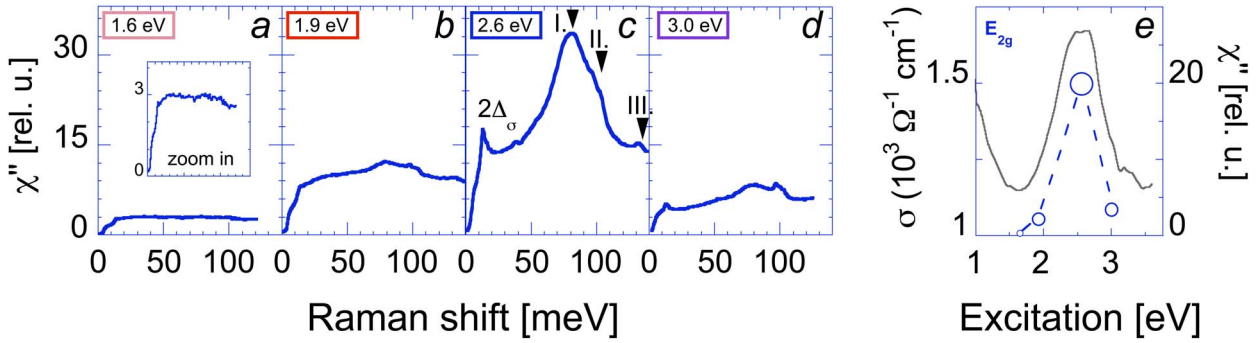

FIG. 1. (Color online) Raman response function from crystal $\mathcal{A}$ at 8 K for *VH* (a) and *RL* (b)–(d) polarizations corresponding to E_{2g} channel for four excitation energies between 1.65 and 3.05 eV. The spectra exhibit a broad electronic continuum, a superconducting coherence peak $2\Delta_\sigma$, the E_{2g} boron stretching phonon mode (I) and two-phonon scattering bands (II and III). The comparison of *ab*-plane optical conductivity (Ref. 19) and the E_{2g} mode intensity is shown in (e). The size of the symbols is proportional to the ratios of mode to electronic background intensity.

and charge-coupled device detector and for optical properties of the material at different wavelengths as described in Ref. 18.

The point group associated with MgB_2 is D_{6h}; subsequently, polarized Raman scattering from the *ab* surface couples to two symmetry channels: E_{2g} and A_{1g}. The corresponding symmetry channels can be resolved if the appropriate light polarization is chosen for the in- and outcoming photons; in this work only the E_{2g} symmetry channel will be discussed. We denote by $(\mathbf{e}_{in}\mathbf{e}_{out})$ a configuration in which the incoming (outgoing) photons are polarized along the $\mathbf{e}_{in}$ ($\mathbf{e}_{out}$) directions. In the *VH* configuration the light is linearly polarized with vertical (*V*) or horizontal (*H*) directions chosen perpendicular or parallel to the crystallographic *a* axis. The "right-left" (*RL*) notation refers to circular polarization: $\mathbf{e}_{in}=(H-iV)/\sqrt{2}$, with $\mathbf{e}_{out}=\mathbf{e}_{in}^*$ for the *RL* geometry. Both the *RL* and the *VH* polarization combinations select the E_{2g} representation.

In Fig. 1 we show the Raman response as a function of excitation energy sampling laser lines $\lambda_L=752.5$, 647.1, 482.5, and 406.7 nm. We chose steps in excitation wavelengths to resolve the broad band at around 2.6 eV in the MgB_2 optical conductivity.[19]

Typical Raman features of E_{2g} symmetry from a MgB_2 single crystal are shown in Fig. 1(c) where phonon modes are designated with arrows. We see that the E_{2g} mode at ~80 meV (I) dominates the Raman response. In addition two-phonon scattering peaks II and III corresponding to flat portions of the phonon dispersion curves at half the frequency of the respective peaks are also observed.[8,20] Finally the spectra exhibit a strong electronic continuum with a SC pair breaking peak at 13.6 meV corresponding to twice the value of the SC gap in the σ bands.[6] The evolution of the pair breaking peak with cooling below T_c is shown in the insets of Figs. 2(a) and 3(a).

The RREP relates Raman scattering intensity to the interband transitions seen in the optical conductivity $\sigma(\omega)$. It is particularly helpful in the visible range because the interband contribution to $\sigma_{ab}(\omega)$ contains a pronounced band around 2.6 eV.[19,21] In Figs. 1(a)–1(d) we show that the intensity of Raman response is in resonance with the 2.6 eV band [Fig. 1(e)]. We note that the ratio of the E_{2g} mode intensity to the strength of the electronic background is also largest around the 2.6 eV excitation. The Raman intensity of the E_{2g} mode is plotted along the right *y* axis in Fig. 1(e) as a function of excitation while the mode intensity to background ratio is represented by the size of the data symbols in the plot. The 2.6 eV peak in optical conductivity is associated with the $\pi\rightarrow\sigma$ electronic transitions in the vicinity of the Γ point and $\sigma\rightarrow\pi$ transitions in the vicinity of the *M* point of the BZ.[1,22,23] The RREP indicates that coupling to the E_{2g} mode is realized via the $\pi\leftrightarrow\sigma$ interband transition. The strongly resonant behavior of the E_{2g} mode places experimental restrictions on how this mode should be investigated.

In Fig. 2(a) Raman spectra for the SC state (zero field) and normal state ($H>H_{c2}$) are juxtaposed, demonstrating the effect of magnetic field applied parallel to the *c* axis at 8 K. The E_{2g} phonon mode hardens below the SC phase transition along with a slight renormalization of its linewidth. At the same time a SC pair breaking peak at 13.6 meV appears indicating the presence of the SC gap. In Fig. 2(b) we demonstrate how the linewidth of the E_{2g} mode monotonically narrows from room temperature down to T_c. To quantify the dependence of the E_{2g} phonon frequency and linewidth as a function of temperature and magnetic field we fitted the data with a sum of phononic oscillators and a SC pair breaking singularity on an electronic background as demonstrated in Fig. 2(a).

In Fig. 3 we evaluate the E_{2g} phonon frequency $\omega_0(T)$ and the damping constant $\Gamma(T)$ for both crystals $\mathcal{A}$ and $\mathcal{B}$ where we distinguish between the respective values for the normal and SC states. The solid line in Fig. 3(b) is a fit of the damping constant $\Gamma(T)$ in the normal state to a model of anharmonic two- and three-phonon decay at one-half and one-third frequencies:

$$\Gamma(T)=\Gamma_0+\Gamma_3[1+2n(\Omega(T)/2)]+\Gamma_4[1+3n(\Omega(T)/3)+3n^2(\Omega(T)/3)]. \quad (1)$$

Here $\Omega(T)=hc\omega_h/k_BT$, with the harmonic frequency $\omega_h=67$ meV,[1,8,23] $n(x)$ is the Bose-Einstein distribution function, Γ_0 is the internal temperature-independent line width of

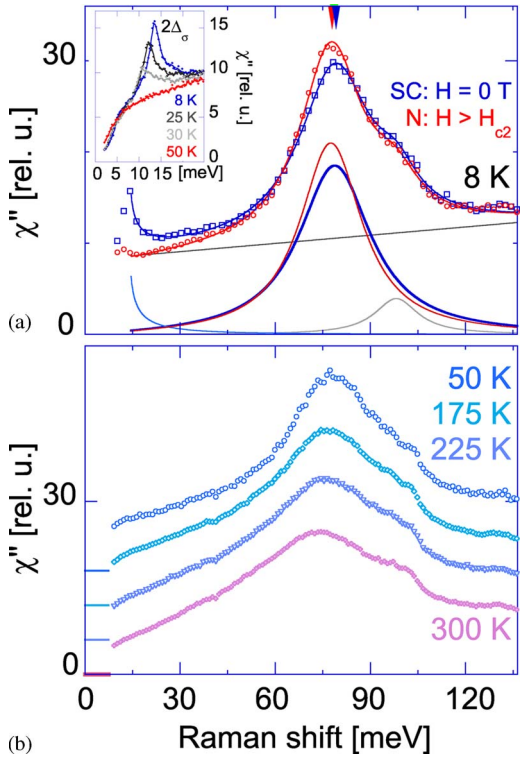

FIG. 2. (Color online) Raman response function in the E_{2g} channel for *RL* polarization and 2.6 eV excitation. (a) Raman response from crystal $\mathcal{B}$ at 8 K. Spectra at zero field and 7 T are compared. Spectra are decomposed into two Raman oscillators, electronic background (linear slope), and coherence peak singularity for the SC state, $\sim[\omega\sqrt{(\omega^2-(2\Delta)^2)}]^{-1}$. The arrows at the top indicate the shift of the E_{2g} mode in the transition from the SC state (blue squares) into the normal state (red circles). Inset: evolution of low-frequency Raman response with temperature across the SC transition. (b) Data from crystal $\mathcal{A}$. Temperature dependence of the E_{2g} phonon mode above T_c. Fit parameters to these spectra are displayed in Fig. 3.

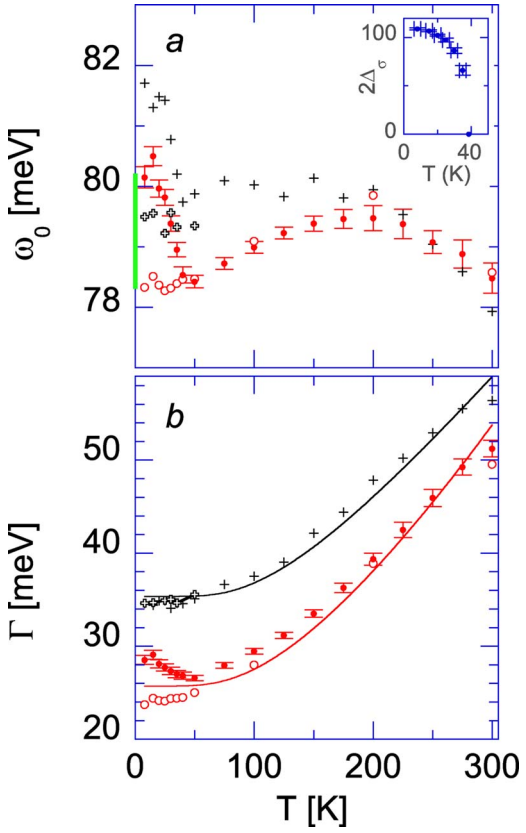

FIG. 3. (Color online) Temperature dependences for the E_{2g} phonon frequency, $\omega_0(T)$ (a), and damping constants, $\Gamma(T)$ (b), for two MgB_2 single crystals $\mathcal{A}$ (black crosses) and $\mathcal{B}$ (red circles) for zero-field cooling (solid symbols) and field cooling at 8 T$>H_{c2}$ (empty symbols). Solid lines are fits of damping constants $\Gamma(T)$ in the normal state with Eq. (1). The parameters from the anharmonic decay fits for both crystals are summarized in Table I. Inset shows temperature dependence of the $2\Delta_\sigma$ coherence peak which follows from the evaluation of spectra shown in the inset to Fig. 2(a). The green bar at the y axis indicates the E_{2g} phonon frequency renormalization upon the SC phase transition.

the phonon, and $\Gamma_{3,4}$ are broadening coefficients due to the cubic and quartic anharmonicities. The results of the fit to this anharmonic decay model are collected in Table I. For both crystals the broadening coefficients $\Gamma_3+\Gamma_4 \gg \Gamma_0$ and therefore the anharmonic decay is primarily responsible for the large damping constant of the E_{2g} phonon. We identify the reason for this rapid phononic decay in the phononic density of states (PDOS) peaking at 33 meV, half of the harmonic E_{2g} phonon frequency ω_h [see Fig. 1(a) in Refs. 3 and 25], which corresponds to the van Hove singularity of the lower acoustic branch (almost dispersionless along the Γ-K-M direction; see Fig. 3 in Ref. 24). In this context the narrowing of the E_{2g} mode with Al substitution observed in Refs. 5 and 24 can be readily explained with the E_{2g} phonon branch moving to energies above 100 meV with increased Al concentration, whereas the acoustic modes that provide the decay channels stay close to their original energies with high PDOS in the energy range of 25–40 meV.[24] In short, the fast decay of the E_{2g} mode is due to the unique combination of its harmonic frequency at the Γ point (67 meV) corresponding to high PDOS at half of this frequency. Thus two independent puzzle pieces; (i) the cubic anharmonicity contribution being much larger than the residual linewidth and (ii) the phonon density peaking just at the right energy to provide suitable decay channels, fit together, giving evidence that the E_{2g} phonon anharmonicity is responsible for the unusually broad linewidth of this mode. In contrast to recent theoretical suggestions[8] current experiment shows that the E_{2g} phonon anharmonicity in MgB_2 must not be neglected. The residual linewidth Γ_0 that we obtain from the fit to the anharmonic decay model, while small, is not in contradiction to theoretical estimates[9,10] of the electron-phonon decay contribution to the E_{2g} phonon linewidth.

It is worth noting that individual Γ_i parameters differ for the two single crystals despite the fact that both samples were grown in the same batch. The E_{2g} mode for crystal $\mathcal{A}$ is by about 10 meV broader than for crystal $\mathcal{B}$. With $\Gamma_0^{\mathcal{A}}$ somewhat higher than $\Gamma_0^{\mathcal{B}}$ and $\Gamma_3^{\mathcal{A}}$ substantially higher than $\Gamma_3^{\mathcal{B}}$ (see Table I) the E_{2g} mode in crystal $\mathcal{A}$ is more anharmonic than in crystal $\mathcal{B}$. Accordingly the crystal $\mathcal{A}$ mode is pushed to about 1.2 meV higher frequency at low temperatures. We

TABLE I. Comparison of T_c and the E_{2g} oscillator parameters for crystals $\mathcal{A}$ and $\mathcal{B}$.

Crystal	T_c[a] (K)	ω_0^N (meV)	ω_0^{SC} (meV)	Γ_0 (meV)	Γ_3 (meV)	Γ_4 (meV)	κ (%)
$\mathcal{A}$	38.2	79.3	81.7	4.0±1.5	31.4±1.2	Small	2.8±0.5
$\mathcal{B}$	38.5	78.1	80.5	Small	22.9±0.7	2.8±0.4	2.3±0.3

[a]From superconducting quantum interferece device measurements at 2 G.

note a correlation between the larger anharmonicity and slightly lower T_c in the case of crystal $\mathcal{A}$.

To describe the superconductivity-induced self-energy effect we refer to Fig. 3(a). Upon cooling in zero field $\omega_0(T)$ exhibits nonmonotonic but smooth behavior down to T_c. Then at T_c it displays abrupt hardening with $\omega_0^{SC}(T)$ scaling to the functional form of the SC gap magnitude $2\Delta_\sigma(T)$ (Fig. 3 inset). For in-field cooling the E_{2g} phonon frequency $\omega_0^N(T)$ remains unrenormalized. The differences between the phonon frequencies in the normal and SC states at 8 K are 2.2±0.4 and 1.8±0.2 meV for crystals $\mathcal{A}$ and $\mathcal{B}$, respectively. To quantify the relative hardening of the E_{2g} mode we obtain the superconductivity-induced renormalization constant $\kappa=(\omega_0^{SC}/\omega_0^N)-1\approx 2.5\%$ (see Table I) which is much smaller than the theoretically predicted $\kappa\approx 12\%$.[13]

We estimate the electron-phonon coupling constant $\lambda_{E_{2g}}^{\Gamma}$ around the BZ center using approximations adopted in Refs. 26 and 27: $\lambda=-\kappa\,\mathrm{Re}[(\sin u)/u]$, where $u\equiv\pi+2i\cosh^{-1}(\omega^N/2\Delta_\sigma)$, and obtain $\lambda_{E_{2g}}^{\Gamma}\approx 0.3$, which is smaller than the theoretically predicted values (compare λ up to unity in Refs. 1, 13, and 28).

In summary, we have measured the polarization-resolved Raman response as a function of excitation energy, temperature, and field for MgB_2 single crystals. From the temperature dependence of the E_{2g} boron stretching phonon we conclude that anharmonic decay is primarily responsible for the anomalously large damping constant of this mode. For this phonon we observe a SC-induced self-energy effect and estimate the electron-phonon coupling constant.

We acknowledge V. Guritanu and A. Kuz'menko for providing optical data, and I. Mazin and W. E. Pickett for valuable discussions. A.M. has been supported in part by the German National Academic Foundation, the Lucent Foundation, and Rutgers University.

*Corresponding author. Email address: girsh@bell-labs.com

[1] J. Kortus, I. I. Mazin, K. D. Belashchenko, V. P. Antropov, and L. L. Boyer, Phys. Rev. Lett. **86**, 4656 (2001).
[2] D. Daghero, R. Gonnelli, G. Ummarino, O. Dolgov, J. Kortus, A. Golubov, and S. Shulga, Physica C **408–410**, 353 (2004).
[3] T. Yildirim *et al.*, Phys. Rev. Lett. **87**, 037001 (2001).
[4] H. Choi, D. Roundy, S. Hong, M. Cohen, and S. Loule, Nature (London) **418**, 758 (2002).
[5] B. Renker, H. Schober, P. Adelmann, P. Bohnen, D. Ernst, R. Heid, P. Schweiss, and T. Wolf, J. Low Temp. Phys. **131**, 411 (2003).
[6] J. W. Quilty, S. Lee, A. Yamamoto, and S. Tajima, Phys. Rev. Lett. **88**, 087001 (2002).
[7] A. Goncharov *et al.*, Phys. Rev. B **64**, 100509(R) (2001).
[8] A. Shukla *et al.*, Phys. Rev. Lett. **90**, 095506 (2003).
[9] M. Calandra and F. Mauri, Phys. Rev. B **71**, 064501 (2005).
[10] E. Cappelluti, Phys. Rev. B **73**, 140505 (2006).
[11] H. J. Choi, D. Roundy, H. Sun, M. L. Cohen, and S. G. Louie, Phys. Rev. B **66**, 020513(R) (2002).
[12] D. Hinks and J. Jorgensen, Physica C **385**, 98 (2003).
[13] A. Y. Liu, I. I. Mazin, and J. Kortus, Phys. Rev. Lett. **87**, 087005 (2001).
[14] L. Boeri, E. Cappelluti, and L. Pietronero, Phys. Rev. B **71**, 012501 (2005).
[15] A. Q. R. Baron, H. Uchiyama, Y. Tanaka, S. Tsutsui, D. T. Ishikawa, S. Lee, R. Heid, and K. Bohnen, Phys. Rev. Lett. **92**, 197004 (2004).
[16] H. Martinho, C. Rettori, P. Pagliuso, A. Martin, N. Moreno, and J. Sarrao, Solid State Commun. **125**, 499 (2003).
[17] J. Karpinski *et al.*, Supercond. Sci. Technol. **16**, 221 (2003).
[18] G. Blumberg, R. Liu, M. V. Klein, W. C. Lee, D. Ginsberg, C. Gu, B. Veal, and B. Dabrowski, Phys. Rev. B **49**, 13295 (1994).
[19] V. Guritanu, A. B. Kuzmenko, D. van der Marel, S. M. Kazakov, N. D. Zhigadlo, and J. Karpinski, Phys. Rev. B **73**, 104509 (2006).
[20] Referring to Fig. 3 of Ref. 8 we read the phonon dispersion to find that the two-phonon peak II results from the A_{2u} branch that is mostly flat all the way along the Γ-*A* line at around 46–47 meV. The E_{2g} optical branch has a minimum at the *A* point at 66 meV resulting in the two-phonon scattering peak III.
[21] A. Kuz'menko *et al.*, Solid State Commun. **121**, 479 (2002).
[22] V. Antropov, K. Belashchenko, M. van Schilfgaarde, and S. Rashkeev, cond-mat/0107123 (unpublished).
[23] I. Mazin and V. Antropov, Physica C **385**, 49 (2003).
[24] K. Bohnen, R. Heid, and B. Renker, Phys. Rev. Lett. **86**, 5771 (2001).
[25] R. Osborn, E. A. Goremychkin, A. I. Kolesnikov, and D. G. Hinks, Phys. Rev. Lett. **87**, 017005 (2001).
[26] R. Zeyher and G. Zwicknagl, Z. Phys. B: Condens. Matter **78**, 175 (1990).
[27] C. O. Rodriguez, A. I. Liechtenstein, I. I. Mazin, O. Jepsen, O. K. Andersen, and M. Methfessel, Phys. Rev. B **42**, 2692 (1990).
[28] A. Golubov *et al.*, J. Phys.: Condens. Matter **14**, 1353 (2002).